Experimental Realization of One-Way Quantum Computing with Two-Photon Four-Qubit Cluster States

Kai Chen,[1,2] Che-Ming Li,[1,3] Qiang Zhang,[2] Yu-Ao Chen,[1] Alexander Goebel,[1] Shuai Chen,[1]
Alois Mair,[1] and Jian-Wei Pan[1,2]

[1]*Physikalisches Institut, Ruprecht-Karls-Universität Heidelberg, Philosophenweg 12, 69120 Heidelberg, Germany*
[2]*Hefei National Laboratory for Physical Sciences at Microscale and Department of Modern Physics,
University of Science and Technology of China, Hefei, Anhui 230026, China*
[3]*Department of Electrophysics, National Chiao Tung University, Hsinchu 30050, Taiwan*
(Received 1 May 2007; published 17 September 2007)

We report an experimental realization of one-way quantum computing on a two-photon four-qubit cluster state. This is accomplished by developing a two-photon cluster state source entangled both in polarization and spatial modes. With this special source, we implemented a highly efficient Grover's search algorithm and high-fidelity two-qubit quantum gates. Our experiment demonstrates that such cluster states could serve as an ideal source and a building block for rapid and precise optical quantum computation.

Highly entangled multipartite states, so-called cluster states, have recently raised enormous interest in quantum information processing (QIP). These sorts of states are crucial as a fundamental resource and a building block aimed at one-way universal quantum computing [1]. They are also essential elements for various quantum error correction codes and quantum communication protocols [2]. Moreover, the entanglements are shown to be robust against decoherence [3], and persistent against loss of qubits [1], and thus are exceptionally well suited for quantum computing and many tasks [1,2]. Considerable efforts have been made toward generating and characterizing cluster state in linear optics [4–9]. Recently the principal feasibility of a one-way quantum computing model has been experimentally demonstrated through 4-photon cluster states successfully [7,8,10].

So far, preparing photonic cluster states still suffers from several serious limitations. Because of the probabilistic nature and Poissonian distribution of the parametric down-conversion process, the generation rate of 4-photon cluster states is quite low [5–8], and largely restricts the speed of computing. Additionally, the quality and fidelity of prepared cluster states are relatively low [6–8], which are difficult to improve substantially. These disadvantages consequently impose great challenges of advancement even for few-qubit quantum computing.

Fortunately, motivated by the fact that an important type of state termed hyperentangled state has been experimentally generated [11–14], we have the possibility to produce a new type of cluster state (2-photon 4-qubit cluster state) with nearly perfect fidelity and high generation rate. The hyperentangled states have been used to test "all-versus-nothing" (AVN) quantum nonlocality [11,12,15] and are shown to lead to an enhancing violation of local realism [16,17]. The states also enable us to perform complete deterministic Bell state analysis [18] as demonstrated in [14,19].

In this Letter we report an experimental realization of one-way quantum computing with such a 2-photon 4-qubit cluster state. The key idea is to develop and employ a bright source which produces a 2-photon state entangled both in polarization and spatial modes. We are thus able to implement the Grover algorithm and quantum gates with excellent performances. The genuine four-partite entanglement and high fidelity of better than 88% are characterized by an optimal entanglement witness. Inheriting the intrinsic two-photon character, our scheme promises a brighter source by 4 orders of magnitude than the usual multiphoton source, which offers a significantly high efficiency for optical quantum computing. It thus provides a simple and fascinating alternative to complement the latter. With ease of manipulation and control, the nearly perfect quality of this source allows us to perform highly faithful and precise quantum computing.

To generate the state we use the technique developed in previous experiments [12] with a type-I spontaneous parametric down-conversion (SPDC) source [20]. The experimental setup is shown in Fig. 1(a). A pulse of ultraviolet (UV) light passes twice through two contiguous beta-barium borate (BBO) with optic axes aligned in perpendicular planes to produce one polarization entangled photon pair, with one possibility in the forward direction with a state $(|H\rangle_A|H\rangle_B + |V\rangle_A|V\rangle_B)/\sqrt{2}$ on spatial (path) modes $L_{A,B}$, and another possibility in the backward direction with a state $(|H\rangle_A|H\rangle_B - |V\rangle_A|V\rangle_B)/\sqrt{2}$ on modes $R_{A,B}$. Here $|H\rangle$ ($|V\rangle$) stands for photons with horizontal (vertical) polarization.

Through perfect temporal overlaps of modes R_A and L_A and of modes R_B and L_B, one can obtain a state

$$\frac{\left[(|H\rangle_A|H\rangle_B + |V\rangle_A|V\rangle_B)|L\rangle_A|L\rangle_B + e^{i\theta}(|H\rangle_A|H\rangle_B - |V\rangle_A|V\rangle_B)|R\rangle_A|R\rangle_B\right]}{2}. \tag{1}$$

By properly adjusting the distance between the concave mirror and the crystal such that $\theta = 0$, the generated state will be exactly the desired cluster state

$$|C_4\rangle = \frac{(|0000\rangle_{1234} + |0011\rangle_{1234} + |1100\rangle_{1234} - |1111\rangle_{1234})}{2}, \tag{2}$$

if we identify the polarization and spatial modes of photon A to be qubits 2,3, respectively, and photon B's polarization and spatial modes to be qubits 1,4 and encode logical qubits as $|H(V)\rangle_B \leftrightarrow |0(1)\rangle_1$, $|H(V)\rangle_A \leftrightarrow |0(1)\rangle_2$, $|L(R)\rangle_A \leftrightarrow |0(1)\rangle_3$, $|L(R)\rangle_B \leftrightarrow |0(1)\rangle_4$. We observe a cluster state generation rate about 1.2×10^4 per second for 200 mW UV pump, which is 4 orders of magnitude brighter than the usual 4-photon cluster state production [6–8] where only a rate of ~1 is achieved per second.

To evaluate the quality of the state, we apply an optimal entanglement witness [21]. The witness is of the form

$$\mathcal{W} = \frac{[4I^{\otimes 4} - (XXIZ + XXZI + IIZZ + IZXX + ZIXX + ZZII)]}{2}, \tag{3}$$

where I is a 2-dimensional identity matrix while $Z = (|0\rangle\langle 0| - |1\rangle\langle 1|)$, $X = (|0\rangle\langle 1| + |1\rangle\langle 0|)$ are Pauli matrices. A negative value for the witness implies 4-partite entan-
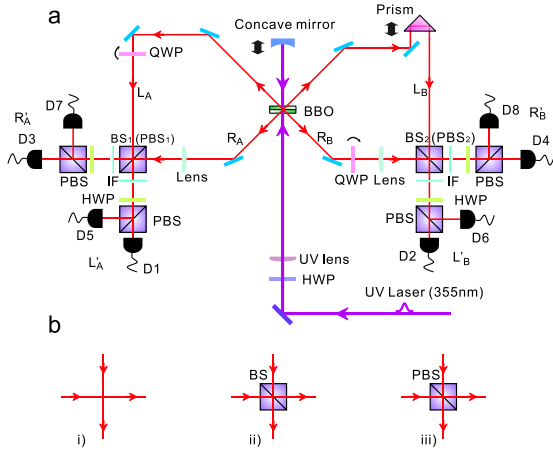

FIG. 1 (color online). Schematic of experimental setup. (a) By pumping a two-crystal structured BBO in a double pass configuration, one polarization entangled photon pair is generated either in the forward direction or in the backward direction. The UV pulsed laser (5 ps) has a central wavelength of 355 nm with a repetition rate of 80 MHz, and an average power of 200 mW. Two quarter wave plates (QWPs) are tilted along their optic axis to vary relative phases between polarization components to attain two desired possibilities for entangled pair creation. Concave mirror and prism are mounted on translation stages to optimize interference on two beam splitters (BS$_{1,2}$) or polarizing beam splitters (PBS$_{1,2}$) for achieving the target cluster state. Half wave plates (HWPs) together with PBS and eight single-photon detectors (D1–D8) are used for polarization analysis of the output state. IFs are 3-nm bandpass filters with central wavelength 710 nm. (b) In the place where BS$_{1,2}$ or PBS$_{1,2}$ are located, three apparatuses are for measuring all necessary observables. Setup (i) is for Z measurement while setup (ii) is used for X measurement for spatial modes. If an α phase shifter is inserted at one of the input modes in (ii) an arbitrary measurement along basis $B(\alpha)$ can be achieved. Setup (iii) can be for Z measurement of spatial mode and, simultaneously, for Z measurement of polarization.

glement for a state close to $|C_4\rangle$ and will be optimally as -1 for a perfect cluster state. Two experimental settings of $XXZZ$ and $ZZXX$ are needed. $XXZZ$ can be attained by measuring in the $+/-$ basis for the polarization in each output arm after apparatus (i) in Fig. 1(b), while $ZZXX$ can be realized by measuring in the H/V basis after apparatus (ii). This is because the beam splitter (BS) acts exactly as a Hadamard transformation for the path modes to change Z basis to X basis for measurement; namely, $|L\rangle_{A,B} \rightarrow (|R'\rangle_{A,B} + |L'\rangle_{A,B})/\sqrt{2}$, $|R\rangle_{A,B} \rightarrow (|R'\rangle_{A,B} - |L'\rangle_{A,B})/\sqrt{2}$. All of the observables for evaluating the witness are listed in Table I. Substituting their experimental values into Eq. (3) yields $\langle\mathcal{W}\rangle_{\exp} = -0.766 \pm 0.004$, which clearly proves the genuine four-partite entanglement by about 200 standard deviations. As shown in [21], one can obtain a lower bound for fidelity of experimental prepared state to $|C_4\rangle$

$$F \geq \tfrac{1}{2} - \tfrac{1}{2}\langle\mathcal{W}\rangle_{\exp} = 0.883 \pm 0.002. \tag{4}$$

This proves to be a better source than the ones in [6–8] where fidelities are about 0.63 [7,8] and 0.74 [6], respectively. We attribute impurity of our state to imperfect overlapping on BS, deviations of BS from 50%, as well as imperfections in the polarization and path modes analysis devices. To get a qualitative depiction for these imperfections, we scan the concave mirror with nanometer displacements and observe interference after BS$_{1,2}$. By measuring along H/V basis in each output arm, we have obtained

TABLE I. Experimental values of all the observable on the state $|C_4\rangle$ for the entanglement witness $\mathcal{W}$ measurement. Each experimental value corresponds to measure in an average time of 1 sec and considers the Poissonian counting statistics of the raw detection events for the experimental errors.

Observable	Value	Observable	Value
$XXIZ$	0.9070 ± 0.0036	$IZXX$	0.9071 ± 0.0037
$XXZI$	0.9076 ± 0.0035	$ZIXX$	0.8911 ± 0.0040
$IIZZ$	0.9812 ± 0.0016	$ZZII$	0.9372 ± 0.0030

visibility of 0.842 ± 0.008, 0.943 ± 0.006, 0.968 ± 0.004, and 0.949 ± 0.006 for coincidences among detectors D1-D2, D1-D4, D3-D2, and D3-D4, respectively.

A cluster state can be represented by an array of nodes where each node is initially in the state of $|+\rangle = (|0\rangle + |1\rangle)/\sqrt{2}$. Every connected line between nodes experiences a controlled-phase (CPHASE) gate acting as $|j\rangle|k\rangle \rightarrow (-1)^{jk}|j\rangle|k\rangle$, $j, k \in \{0, 1\}$ [1]. For a given cluster state, consecutive single-qubit measurements in basis $B_k(\alpha) = \{|\alpha_+\rangle_k, |\alpha_-\rangle_k\}$ will define a quantum computing in addition to feed forward of measurement outputs, where $|\alpha_\pm\rangle_k = (|0\rangle \pm e^{i\alpha}|1\rangle)_k/\sqrt{2}$ ($\alpha \in \mathbb{R}$). A measurement output of $|\alpha_+\rangle_k$ means "0" while $|\alpha_-\rangle_k$ signifies "1." This measurement basis determines a rotation $R_z(\alpha) = \exp(-i\alpha Z/2)$, followed by a Hadamard operation $H = (X + Z)/\sqrt{2}$ of encoded qubits. The state $|C_4\rangle$ can be represented by a box-type graph shown in Fig. 2(a), up to a local unitary transformation.

Grover's algorithm.—For an unsorted database with N entries, Grover's search algorithm gives a quadratic speed up for $\sim\sqrt{N}$ consultations on average [22]. Striking linear optics implementations have been achieved in [23,24], although it is questionable whether the algorithm is truly "quantum" due to a demonstration [24] based on interference of classical waves. One-way realizations have been carried out [7,8] recently. In the case of four entries $|00\rangle$, $|01\rangle$, $|10\rangle$, $|11\rangle$, a single quantum search will find the marked element An execution goes as follows: an oracle encodes a desired entry by changing its sign through a black box with initial state $|++\rangle$. After an inversion-about-the-mean operation, the labeled element will be found with certainty by readout. It is shown in [7] that this can be exactly finished with the box cluster state in Fig. 2(a). For demonstration, we experimentally tag the element $|00\rangle$ on qubits 2,3 and make the readout on qu-
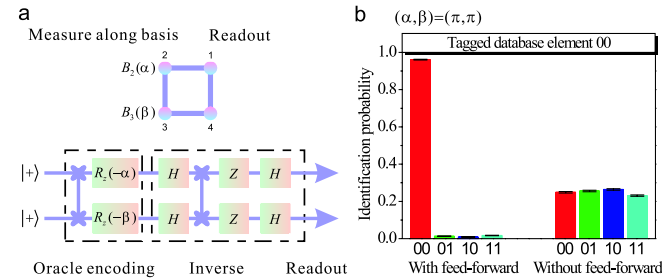
bits 1,4 all along basis $B(\pi)$. Because of the fact that the state Eq. (2) distinguishes the box cluster from an H transformation on every qubit and a swap between qubits 2 and 3, this amounts to measuring along the V/H basis after apparatus (iii) in Fig. 1(b). Two polarizing beam splitters (PBS) here are for interfering, to ensure the desired cluster state. In the meantime they are acting as polarization measurement devices, which is equivalent to using apparatus (i) in this case. The outputs of the algorithm are 2 bits $\{s_3 \oplus s_4, s_1 \oplus s_2\}$ in lab basis by feed forwarding outcomes of qubits 2,3, where s_i are measurement outcomes on qubits i. The experimental results are sketched in Fig. 2(b).

Quantum gates.—Nontrivial two-qubit quantum gates such as the CPHASE gate are at the heart of universal quantum computation that can be realized by cluster states conveniently. Depending on the initial cluster state and measurement basis, states with different degrees of entanglement can be generated. The horseshoe or box cluster shown in Figs. 3(a) and 3(c) can realize such important gates. For the case of horseshoe cluster in Fig. 3(a), depending on the outcomes when measuring along basis $B_2(\alpha)$ and $B_3(\beta)$, the output state on qubits 1,4 would be $|\Omega_{\text{out}}\rangle = (X^{s_2} \otimes X^{s_3})(H \otimes H)(R_z(-\alpha) \otimes R_z(-\beta))\text{CPhase}|\Omega_{\text{in}}\rangle$, where $|\Omega_{\text{in}}\rangle = |++\rangle$. The state $|\Omega_{\text{out}}\rangle$ is always a maxi-

FIG. 2 (color online). Demonstration of Grover's algorithm. (a) Equivalent quantum circuit of Grover's algorithm using box cluster state. The "oracle" encodes the element "00" by measuring along basis $B_{2,3}(\pi)$, while the inverse and readout sections will find this entry with certainty by a single query. (b) A successful identification probability of $(96.1 \pm 0.2)\%$ is achieved deterministically with feed forward, while it is $(24.9 \pm 0.4)\%$ without feed forward. This is in excellent agreement with theoretical expectations. The trick is that the black box provides only outcomes but not basis information for feed forward. Thus the oracle encoding is hidden before feed forward on readout.
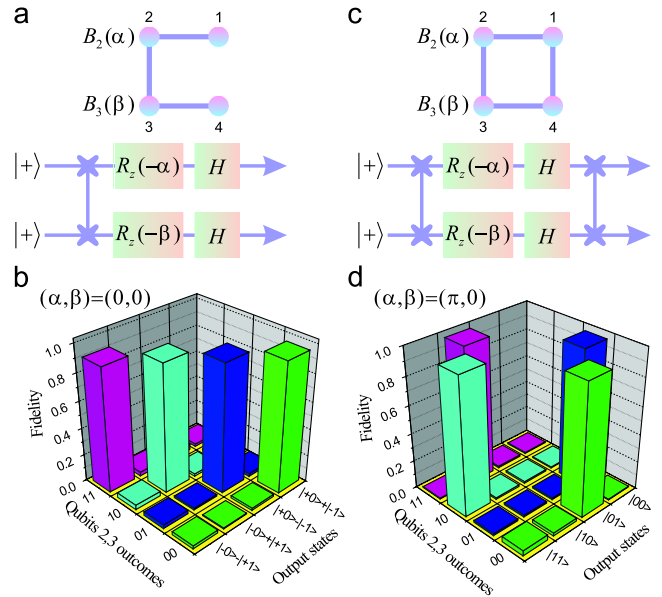

FIG. 3 (color online). Two-qubit quantum gate realizations. (a) CPHASE gate realization with the horseshoe cluster. (b) Experimental measured fidelities of output states to the ideal Bell states (unnormalized) in the lab basis. They are 0.954 ± 0.003, 0.940 ± 0.004, 0.936 ± 0.005, 0.910 ± 0.005 for outcomes 00, 01, 10, 11 on qubits 2,3, respectively. (c) Quantum gate implementation that does not generate entanglement with the box cluster. (d) Measured fidelities of output states to the ideal product states in the lab basis. They are 0.935 ± 0.005, 0.962 ± 0.004, 0.969 ± 0.003, 0.975 ± 0.003 for outcomes 00, 01, 10, 11 on qubits 2,3, respectively.

mal entangled state, taking $\alpha = \beta = 0$ and considering outcomes "00" in qubits 2,3. This implies a final Bell state of $|\Omega_{\text{out}}\rangle = (|+\rangle|0\rangle + |-\rangle|1\rangle)/\sqrt{2}$. Note that the horseshoe cluster state is equivalent to the state Eq. (3) up to a $HIIH$ transformation, in lab basis this amounts to the fact that the output state is exactly $|\Omega_{\text{out}}\rangle$, which is symmetric under HH transformation. To characterize the quality of quantum gate outputs, we put a birefringent crystal in path R_B to make a transformation $|+\rangle \leftrightarrow |-\rangle$ for polarization. After BS$_2$, all the Bell states on qubits 1,4 will change as

$$(|+\rangle_1|0\rangle_4 \pm |-\rangle_1|1\rangle_4)/\sqrt{2} \rightarrow |+\rangle_1|\pm\rangle_4,$$
$$(|-\rangle_1|0\rangle_4 \pm |+\rangle_1|1\rangle_4)/\sqrt{2} \rightarrow |-\rangle_1|\pm\rangle_4, \tag{5}$$

which can be completely and deterministically discriminated by measuring along $|\pm\rangle$ basis. The fidelities of the output states in the lab basis to the ideal Bell state are shown in Fig. 3(b). Similarly, for the box cluster state shown in Fig. 3(c), measurements on qubits 2,3 along basis $\{B_2(\alpha), B_3(\beta)\}$ will give an output state on qubits 1,4 with $|\Omega_{\text{out}}\rangle = (Z \otimes X)^{s_3}(X \otimes Z)^{s_2}\text{CPhase}(H \otimes H)(R_z(-\alpha) \otimes R_z(-\beta))\text{CPhase}|\Omega_{\text{in}}\rangle$, which is a product state when $\alpha = \pi$ and $\beta = 0$. Since we can completely distinguish 4 different products states, output fidelities can be obtained directly, as shown in Fig. 3(d). By employing the techniques developed in [8] with active feed forward, one can expect to achieve deterministically quantum computing with excellent quality outputs.

We remark that other 2-qubit states can be generated by suitable measurements on qubits 2,3. However, an arbitrary single-qubit rotation needs generally 3 single-qubit measurements on a cluster for one-way implementation [7,8], which is a big consumption of resources. Fortunately, this rotation can be easily attained by linear optical components both for polarization and spatial modes. Therefore a hybrid framework would be more practical with one-way realization of two-qubit gates and the usual single-qubit gates. Because of low efficiency for producing multiphoton and concurrent occupations for polarization-spatial degrees of freedom of the photons, our source is not yet scalable, the same as the multiphoton source [8]. However, the scheme developed here leads to quantum computing with a quality and efficiency at present largely unmatched by previous methods.

In summary, we have developed a scheme for preparation of a 2-photon 4-qubit cluster state and designed and demonstrated the first proof-of-principle realization of one-way quantum computing employing such a source. The excellent quality of the state with fidelity better than 88% is achieved. The high count rates enable quantum computing 4 orders of magnitude more efficient than previous methods. We have implemented the Grover algorithm with a successful probability of about 96% and quantum gates with high fidelities of about 95% on average. Our scheme helps to make a significant advancement of QIP, and the source constitutes a promising candidate

for efficient and high quality one-way optical quantum computing. By using more photons and more degrees of freedom, one can expand our ability to generate many-qubit cluster states for performing quantum computing and other complex tasks. Our results can also find rapid applications in quantum error correction codes, multipartite quantum communication protocols [2], as well as novel types of AVN tests for nonlocality [15].

Note added.—During preparation of our manuscript, we were made aware of one related experiment for realization of a linear cluster state [25].

[1] H. J. Briegel and R. Raussendorf, Phys. Rev. Lett. **86**, 910 (2001); R. Raussendorf and H. J. Briegel, *ibid.* **86**, 5188 (2001); R. Raussendorf, D. E. Browne, and H. J. Briegel, Phys. Rev. A **68**, 022312 (2003).
[2] D. Schlingemann and R. F. Werner, Phys. Rev. A **65**, 012308 (2001); R. Cleve, D. Gottesman, and H.-K. Lo, Phys. Rev. Lett. **83**, 648 (1999).
[3] M. Hein, W. Dür, and H.-J. Briegel, Phys. Rev. A **71**, 032350 (2005).
[4] D. E. Browne and T. Rudolph, Phys. Rev. Lett. **95**, 010501 (2005); T. P. Bodiya and L.-M. Duan, *ibid.* **97**, 143601 (2006).
[5] P. Walther, M. Aspelmeyer, K. J. Resch, and A. Zeilinger, Phys. Rev. Lett. **95**, 020403 (2005).
[6] N. Kiesel *et al.*, Phys. Rev. Lett. **95**, 210502 (2005).
[7] P. Walther *et al.*, Nature (London) **434**, 169 (2005).
[8] R. Prevedel *et al.*, Nature (London) **445**, 65 (2007).
[9] C.-Y. Lu *et al.*, Nature Phys. **3**, 91 (2007).
[10] M. S. Tame *et al.*, Phys. Rev. Lett. **98**, 140501 (2007).
[11] C. Cinelli *et al.*, Phys. Rev. Lett. **95**, 240405 (2005).
[12] T. Yang *et al.*, Phys. Rev. Lett. **95**, 240406 (2005).
[13] J. T. Barreiro, N. K. Langford, N. A. Peters, and P. G. Kwiat, Phys. Rev. Lett. **95**, 260501 (2005).
[14] C. Schuck, G. Huber, C. Kurtsiefer, and H. Weinfurter, Phys. Rev. Lett. **96**, 190501 (2006).
[15] A. Cabello, Phys. Rev. Lett. **87**, 010403 (2001); Z.-B. Chen *et al.*, *ibid.* **90**, 160408 (2003).
[16] A. Cabello, Phys. Rev. Lett. **97**, 140406 (2006).
[17] M. Barbieri *et al.*, Phys. Rev. Lett. **97**, 140407 (2006).
[18] P. G. Kwiat and H. Weinfurter, Phys. Rev. A **58**, R2623 (1998).
[19] M. Barbieri, G. Vallone, P. Mataloni, and F. De Martini, Phys. Rev. A **75**, 042317 (2007).
[20] P. G. Kwiat *et al.*, Phys. Rev. A **60**, R773 (1999).
[21] G. Tóth and O. Gühne, Phys. Rev. A **72**, 022340 (2005).
[22] L. K. Grover, Phys. Rev. Lett. **79**, 325 (1997).
[23] P. G. Kwiat, J. R. Mitchell, P. D. D. Schwindt, and A. G. White, J. Mod. Opt. **47**, 257 (2000).
[24] N. Bhattacharya, H. B. van Linden van den Heuvell, and R. J. C. Spreeuw, Phys. Rev. Lett. **88**, 137901 (2002).
[25] G. Vallone *et al.*, Phys. Rev. Lett. **98**, 180502 (2007).